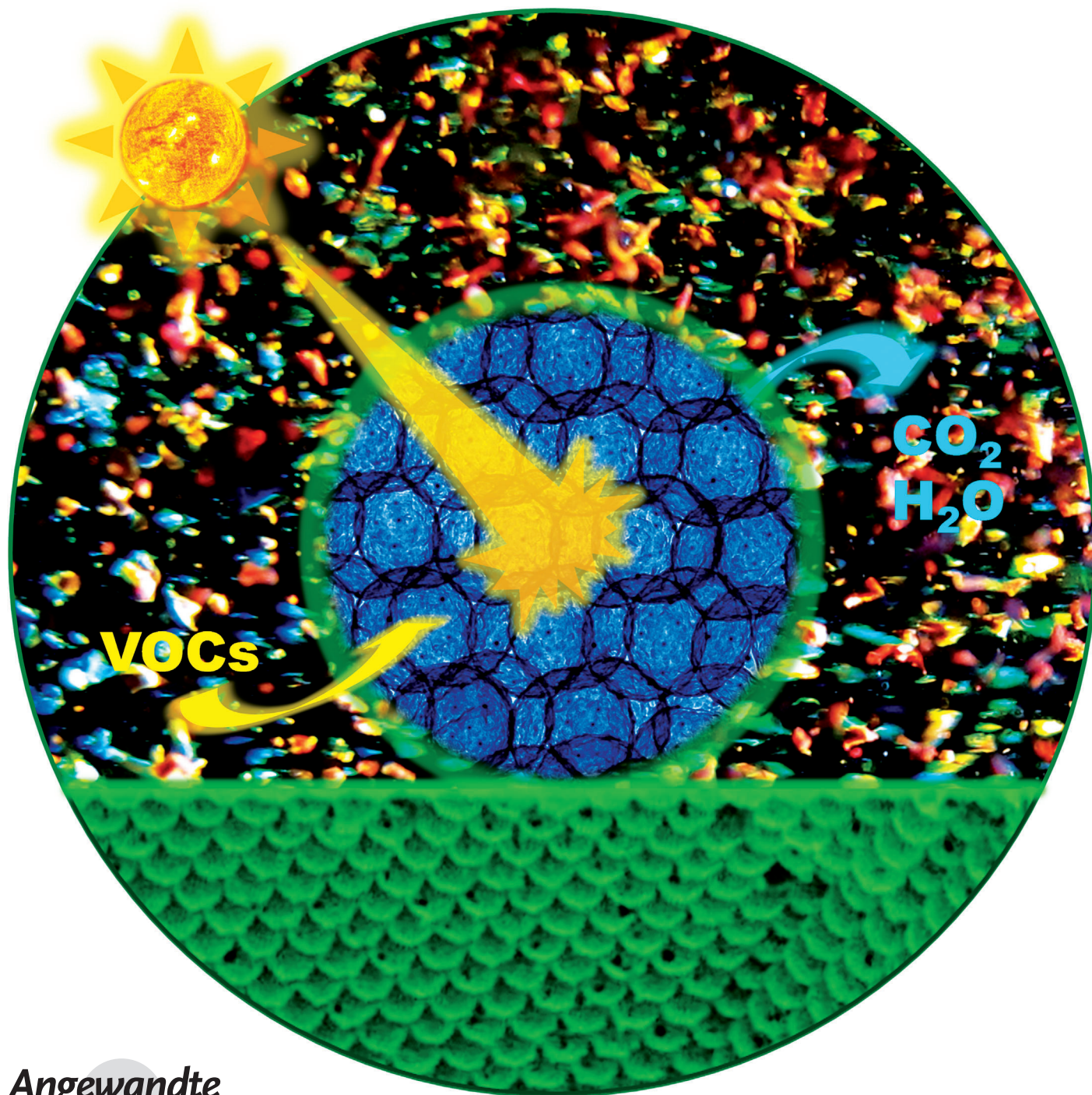


Three-Dimensional Ordered Assembly of Thin-Shell Au/TiO₂ Hollow Nanospheres for Enhanced Visible-Light-Driven Photocatalysis**

Cao-Thang Dinh, Hoang Yen, Freddy Kleitz, and Trong-On Do*



Abstract: An Au/TiO₂ nanostructure was constructed to obtain a highly efficient visible-light-driven photocatalyst. The design was based on a three-dimensional ordered assembly of thin-shell Au/TiO₂ hollow nanospheres (Au/TiO₂-3 DHNSs). The designed photocatalysts exhibit not only a very high surface area but also photonic behavior and multiple light scattering, which significantly enhances visible-light absorption. Thus Au/TiO₂-3 DHNSs exhibit a visible-light-driven photocatalytic activity that is several times higher than conventional Au/TiO₂ nanopowders.

Visible-light-driven photocatalysis for hydrogen production and degradation of pollutants has attracted a tremendous amount of interest over the past decades as it offers direct use of sunlight for energy and environmental applications.^[1] Among many photocatalysts developed to date, TiO₂ is considered to be the most suitable candidate for commercial scale-up because it is abundant, nontoxic, and stable under photochemical conditions.^[2] However, its large band gap means that TiO₂ is only active in the ultraviolet (UV) region, which accounts for less than 5% of the total energy of the solar spectrum. Strategies have been proposed to expand the TiO₂ optical absorption spectrum into the visible region, which accounts for 43% of the solar spectrum, including sensitizing TiO₂ with dyes or small-band-gap quantum dots,^[3] and doping TiO₂ with metal or nonmetal elements.^[4] Recently, a new approach for enhancing the visible light photoactivity of TiO₂ by the plasmonic effect of metal nanostructures has received much attention.^[5] Under visible-light illumination, plasmon-excited hot electrons in noble-metal nanoparticles (NPs) can be transferred to the conduction band of an adjacent semiconductor, and then participate in subsequent chemical reactions.^[5e,f,i] Among various plasmonic metals, Au is the most studied owing to its high stability and strong visible-light absorption over a wide range. As a consequence, several Au/TiO₂ composite systems have been developed for solar water splitting and photocatalytic conversion of organic compounds.^[5j]

Traditional methods for designing Au/TiO₂ photocatalysts mainly focus on improving the dispersion of Au NPs and the surface area of TiO₂ matrix.^[5j,k] Although the photocatalytic activity can be improved because of the higher density of active sites, these Au/TiO₂ materials usually exhibit low

visible-light absorption because of the limited contribution of TiO₂, which absorbs only UV light. On the other hand, incorporation of Au NPs in photonic structures was found to enhance the surface plasmon resonance of Au NPs.^[6] Materials with photonic structures exhibit the slow photon effect, in which light propagates in the material with extremely low group velocities. When the slow photon wavelength overlaps with the light that the material can absorb, an enhanced light absorption can be obtained.^[7] The slow photon effect has also been demonstrated to enhance light absorption of semiconductors, such as TiO₂,^[7c-f] ZnO,^[7i] WO₃,^[7h] or TaON,^[7j] and consequently, increase their photocatalytic activities. Combining Au NPs and TiO₂ that possess a photonic structure would thus be a promising strategy to obtain efficient visible-light-driven photocatalysts. To date, TiO₂ photocatalysts with photonic properties are primarily based on ordered macroporous structures.^[7c-f,8] However, these ordered macroporous TiO₂ materials have a relatively low surface area compared to their nanoparticle or mesoporous counterparts, which prevents them from being efficient photocatalysts.

Herein, we report on a novel Au/TiO₂ nanostructured photocatalyst that is constructed by the three-dimensional ordered assembly of thin-shell Au/TiO₂ hollow nanospheres (namely Au/TiO₂-3 DHNSs). The designed materials exhibit not only exceedingly high surface area but also photonic behavior originating from periodic macroscopic voids from both the inside and the outside of hollow spheres that have very thin shells. The multiple light scattering and slow photon effects resulting from this unique architecture greatly enhance the surface plasmon resonance of Au NPs, which leads to a significant enhancement in the visible light absorption of Au/TiO₂-3 DHNSs. As a result, these new photocatalysts exhibit a photocatalytic activity that is several times higher than conventional Au/TiO₂ nanopowders, as illustrated by the example of the photocatalytic decomposition of isopropanol under visible-light illumination.

To synthesize Au/TiO₂-3 DHNSs, uniform titanate nanodisks (TNDs)^[9] as titania precursors were first coated onto the surface of SiO₂ nanospheres (NSs) using a layer-by-layer technique and poly(ethyleneimine) (PEI) as a polyelectrolyte, to produce TND-PEI/SiO₂ NSs (Figure 1). The layer-by-layer technique combined with the uniform size of TNDs allows the formation of a homogeneous and tunable shell thickness, which is crucial for the formation of 3D ordered assembly structures. The Au precursors (AuCl₄⁻) were then loaded on TND-PEI/SiO₂ NSs to form TND-PEI-AuCl₄⁻/SiO₂ NSs. The

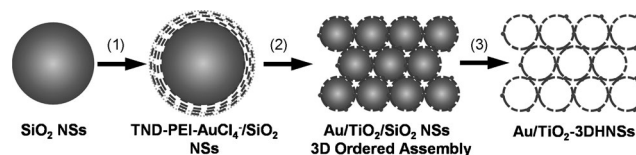


Figure 1. Schematic illustration of the procedure for the design of Au/TiO₂-3 DHNSs: 1) Uniform coating of TNDs on the surface of colloidal SiO₂ NSs followed by the loading of AuCl₄⁻ to form TND-PEI-AuCl₄⁻/SiO₂; 2) assembly of TND-PEI-AuCl₄⁻/SiO₂ into a 3D ordered structure followed by calcination to form a 3D ordered assembly of Au/TiO₂/SiO₂; 3) removal of SiO₂ to obtain Au/TiO₂-3 DHNSs.

[*] C.-T. Dinh, Prof. T.-O. Do
Department of Chemical Engineering and Centre de recherche sur les propriétés des interfaces et la catalyse (CERPIC)
Université Laval, Québec, G1V 0A6 (Canada)
E-mail: trong-on.do@gch.ulaval.ca

H. Yen, Prof. F. Kleitz
Department of Chemistry and
Centre de recherche sur les matériaux avancés (CERMA)
Université Laval, Québec, G1V 0A6 (Canada)

[**] This work was supported by the Natural Sciences and Engineering Research Council of Canada (NSERC). C.T.D. thanks the FQRNT for the Excellence Scholarship. F.K. thanks Yongbeom Seo and Prof. Ryong Ryoo (KAIST, Korea) for access to high-resolution TEM microscopy data.

Supporting information for this article is available on the WWW under <http://dx.doi.org/10.1002/anie.201400966>.

strong interaction between AuCl_4^- and the amine groups^[10] in PEI enables a homogeneous deposition of the Au precursor on each TND-PEI/ SiO_2 NS. The obtained NSs were then packed into 3D ordered assembly structure using a centrifugation process, and then calcined at 550°C to convert AuCl_4^- and TNDs into Au and TiO_2 , respectively. Finally, the SiO_2 NSs core was removed by dissolving the product in a solution of NaOH to obtain Au/ TiO_2 3DHNSs.

Figure 2 A and Figure S1 in the Supporting Information show transmission electron microscopy (TEM) images of TND-PEI- $\text{AuCl}_4^-/\text{SiO}_2$ NSs obtained by coating TNDs on

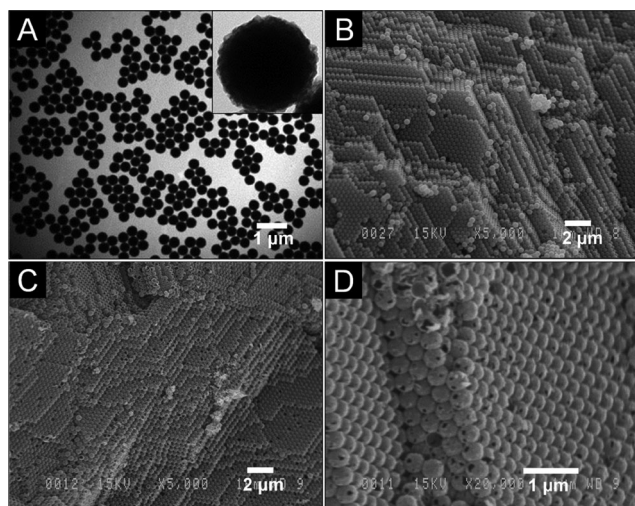


Figure 2. A) TEM image of TND-PEI- $\text{AuCl}_4^-/\text{SiO}_2$ NSs (inset shows a high-magnification image); B) SEM image of 3D ordered assembly of Au- $\text{TiO}_2/\text{SiO}_2$; C, D) SEM images of Au/ TiO_2 -3DHNSs.

SiO_2 NSs, followed by loading of AuCl_4^- . The NSs are highly uniform in size with a diameter of 370 nm. Compared to bare SiO_2 NSs (Figure S2), the surface of TND-PEI- $\text{AuCl}_4^-/\text{SiO}_2$ NSs became rougher (see insert in Figure 2 A), thus indicating the successful deposition of TNDs on the surface of SiO_2 . Figure 2B shows a scanning electron microscopy (SEM) image of 3D ordered assembly of Au/ $\text{TiO}_2/\text{SiO}_2$ NSs obtained by packing of the TND-PEI- $\text{AuCl}_4^-/\text{SiO}_2$ using centrifugation, followed by calcination at 550°C . It can be seen that the NSs were packed into a face-centered-cubic structure that is visible over a wide range. Interestingly, this 3D ordered assembly structure was retained after removal of the SiO_2 cores to obtain hollow nanospheres (HNSs; Figure 2C and D). The high-magnification SEM image of Au/ TiO_2 -3DHNSs (Figure 2D) shows some broken particles which clearly indicates the hollow structure of the NSs. Furthermore, the presence of holes on the shell of each HNS is also observed. These holes might be formed during the removal of the SiO_2 cores. The presence of these holes, in fact, will be beneficial for the photocatalytic application as they enhance the diffusion of the reactants through the shell of the HNSs (vide infra).

Figure S3 in the Supporting Information shows X-ray diffraction (XRD) pattern of Au/ TiO_2 -3DHNSs that corrob-

orates the formation of the anatase phase of TiO_2 . In addition, the presence of diffraction peak at 44.3° , corresponding to the (200) plane of Au, is also seen, which confirms the presence of crystalline Au. The composition of Au/ TiO_2 -3DHNSs determined by energy dispersive X-ray spectroscopy (EDX; Figure S4) shows the presence of 3.5 wt% of Au in the composite.

The morphology of the Au/ TiO_2 -3DHNSs was further characterized by TEM and STEM (Figure 3). It is clearly seen that the sample is an assembly of uniform HNSs (Figure 3 A). The STEM and high-magnification TEM images (Figure 3 B and C) show Au NPs that are evenly distributed on the wall of

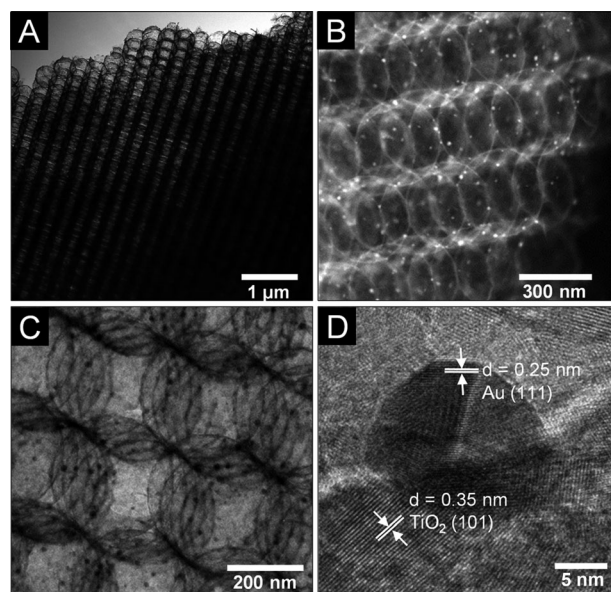


Figure 3. A) TEM; B) STEM; C, D) HRTEM images of Au/ TiO_2 -3DHNSs.

TiO_2 HNSs with an average size of around 12 nm. The thickness of the HNS shell is approximately 10 nm. The high-resolution TEM image (Figure 3D) shows the lattice fringes of both TiO_2 and Au, thus indicating the highly crystalline nature of TiO_2 shell and Au NPs. The lattice fringe with a d-spacing of 0.35 nm can be assigned to the (101) lattice plane of anatase TiO_2 , and the fringe with a d-spacing of 0.25 nm belongs to the (111) lattice plane of Au with a face-centered-cubic phase. Figure 3D also shows the presence of intimate contacts between Au and TiO_2 . This close contact between metal and semiconductor may enhance the charge transfer between them, and thus the photocatalytic efficiency.^[5d]

The surface chemical states of Au and Ti were characterized by X-ray photoelectron spectroscopy (XPS). As shown in Figure S5 in the Supporting Information, the peak observed at a binding energy of 83.3 eV was ascribed to metallic Au $4f_{7/2}$, thus confirming that the Au species exist as metallic Au⁰ in Au/ TiO_2 -3DHNSs.^[6b,11] Compared to bulk Au ($4f_{7/2}$ at 84.0 eV), the Au $4f_{7/2}$ peak in Au/ TiO_2 -3DHNSs exhibits a negative shift of 0.7 eV, which could be due to electron transfer from the oxygen vacancies of TiO_2 to Au that leads to a lower binding energy of Au $4f_{7/2}$ in Au/ TiO_2 -

3DHNSs.^[11] The Ti 2p_{3/2} XPS spectrum of TiO₂ (Figure S6) shows a peak at a binding energy of 458.4 eV, which could be identified as that of Ti⁴⁺ from anatase TiO₂.^[12] The porous structure of the Au/TiO₂-3DHNSs was characterized using N₂ physical adsorption at -196 °C. As shown in Figure S7, the pore size distribution calculated by applying the nonlocal density functional theory method on the adsorption branch reveals maxima in the range 3–12 nm, indicating a porous shell of Au/TiO₂ HNSs.^[13] The specific surface area of the composite reaches 200 m²g⁻¹, which is several times higher than conventional ordered macroporous TiO₂ (often in the range 20–40 m²g⁻¹),^[7f,k,8a] and is comparable to most high-surface-area TiO₂ materials.^[14]

The optical properties of Au/TiO₂-3DHNSs were investigated using diffuse reflectance UV/Vis spectroscopy with TiO₂-3DHNSs as reference sample. As shown in Figure 4A,

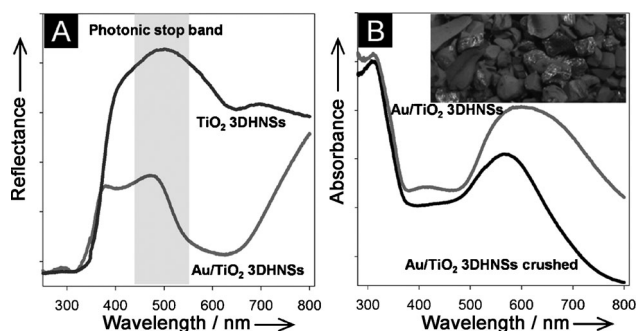


Figure 4. A) UV/Vis diffuse reflectance spectra for Au/TiO₂ 3DHNSs and the TiO₂-3DHNSs reference sample. The shaded region in (A) shows the presence of photonic stop band. B) UV/Vis absorption spectra of Au/TiO₂-3DHNSs before and after being crushed. Inset in (B) shows a digital photo of Au/TiO₂-3DHNSs.

the reflection spectra for both samples begin to attenuate sharply as the wavelength becomes shorter than 380 nm. This behavior is caused by strong intrinsic absorption of light in the anatase TiO₂ semiconductor. In the case of Au/TiO₂-3DHNSs, another decrease in reflection spectrum centered at 580 nm is due to the surface plasmon resonance of Au NPs. Interestingly, both samples exhibit photonic behavior as evidenced by the presence of Bragg reflection peaks centered at around 490 nm. The slow photon effect that occurs at the edges of the stop band is expected to appear in the range 550–620 nm for Au/TiO₂-3DHNSs, which matches well with the absorption spectrum of Au NPs. The wavelength matching of surface plasmon resonance absorption and photonic band edge would be expected to increase the surface plasmon resonance intensity because an increase of the effective path length of light in the photonic band edge regions would result in a significant enhancement of the interaction between photons and Au NPs.

To confirm that the 3DHNS structure has an enhancement effect on the light harvesting, the absorption spectrum of Au/TiO₂-3DHNSs sample and that of the same material, but crushed in an agate mortar to completely destroy the 3DHNS structure (Figure S8 in the Supporting Information), were analyzed (Figure 4B). It is clearly seen that, the

uncrushed sample exhibits an enhanced light absorption, especially in the range 500–800 nm, compared to the crushed sample. In fact, the UV/Vis absorption spectrum of the crushed Au/TiO₂-3DHNSs appeared to be similar to that of conventional Au NPs dispersed on commercial titanium dioxide, P25 Degussa, 3.5 wt % of Au (Au/TiO₂-P25; Figure S9). The result confirms that the macroporous structure plays a crucial role in visible light absorption enhancement. Furthermore, it is also noted that the light absorption enhancement of the uncrushed sample compared to the crushed one occurs not only in the photonic-band-edge region (550–620 nm), but in the whole range of the UV/Vis region. This result indicates that, beside the slow photon effect, the multiple light scattering is also important for the light absorption enhancement. The inset in Figure 4B shows a digital photo of the Au/TiO₂-3DHNS that shows several colors. These colors result from the light reflectance on different planes of the Au/TiO₂-3DHNS particles that originates from the photonic behavior of the materials.^[15]

The photocatalytic activity of Au/TiO₂-3DHNSs was investigated in the photocatalytic decomposition of isopropanol to CO₂ under visible-light illumination ($\lambda \geq 420$ nm). Figure 5A shows the amount of CO₂ generated during the

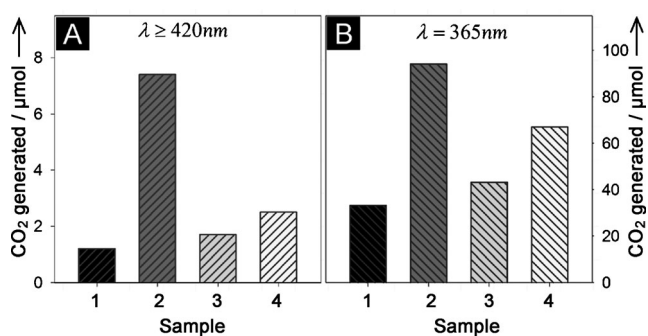


Figure 5. Amount of CO₂ generated A) under visible-light illumination ($\lambda \geq 420$ nm) for 10 h and B) under UV-light illumination ($\lambda = 365$ nm) for 4 h using 1) Au/TiO₂-P25, 2) Au/TiO₂-3DHNSs, 3) crushed Au/TiO₂-3DHNSs, 4) Au/TiO₂-HNSs (without the 3D ordered structure) as photocatalysts.

course of 10 h of visible light illumination using Au/TiO₂-3DHNSs and Au/TiO₂-P25 as a reference sample. It can be seen that Au/TiO₂-3DHNSs can produce 7.4 μ mol of CO₂, which is 6.1 times higher than that produced by Au/TiO₂-P25 (1.2 μ mol) under the same reaction conditions. The excellent photocatalytic activity of Au/TiO₂-3DHNSs under visible light is attributed to the novel nanostructure.

To confirm the effects of the structure on the photocatalytic properties, we evaluated the photocatalytic activities of the crushed Au/TiO₂-3DHNSs and Au/TiO₂-HNSs without the 3D ordered structure (Figure S10 in the Supporting Information). As shown in Figure 5A, the photocatalytic activity of the crushed Au/TiO₂-3DHNSs sample was significantly lower than that of the uncrushed sample. The crushed Au/TiO₂-3DHNSs sample produced 1.7 μ mol of CO₂ after 10 h of reaction, which is 4.3 times smaller than the uncrushed sample, even though this crushed sample has a slightly higher

surface area ($210 \text{ m}^2 \text{ g}^{-1}$) than that of the uncrushed sample ($200 \text{ m}^2 \text{ g}^{-1}$). Although the photocatalytic activity of the crushed Au/TiO₂-3DHNSs is significantly reduced, it is still 1.4 times higher than that of Au/TiO₂-P25. The higher activity of the crushed sample might be due to its higher surface area ($210 \text{ m}^2 \text{ g}^{-1}$) as compared to that of Au/TiO₂-P25 (around $50 \text{ m}^2 \text{ g}^{-1}$). As also seen in Figure 5 A, Au/TiO₂-HNSs (e.g., without the 3D ordered structure) can generate 2.5 μmol of CO₂ which is 1.5 times higher than that produced by crushed Au/TiO₂-3DHNSs under the same conditions. However, compared to that of Au/TiO₂-HNSs with the 3D ordered assembly structure, the photocatalytic activity of Au/TiO₂-HNSs without 3DNSs is 3 times lower. These results reveal that not only the hollow structure but also the 3D ordered assembly structure play an important role for the enhancement of the photocatalytic activity. The 3D ordered assembly of HNSs with periodic voids exhibits the slow photon effect which enhances the visible light absorption, and as a consequence, increases the photocatalytic activity of Au/TiO₂-3DHNSs.

To study the effect of light scattering on the photocatalytic activity of Au/TiO₂-3DHNSs, the photocatalytic experiments were carried out using UV light (365 nm). This wavelength is far below the stop band of the Au/TiO₂-3DHNSs, thus the slow photon effect is not expected.^[7c] Under these reaction conditions, TiO₂ is capable of adsorbing the UV light and generating electrons and holes for the photocatalytic decomposition of isopropanol. As seen in Figure 5 B, the Au/TiO₂-3DHNSs can produce 94.1 μmol of CO₂ which is 2.8, 2.1, and 1.4 times higher than the amount of CO₂ produced by Au/TiO₂-P25 (33.1 μmol), crushed Au/TiO₂-3DHNSs (43.2 μmol), and Au/TiO₂-HNSs (67.3 μmol), respectively. The crushed and uncrushed Au/TiO₂-3DHNSs samples and Au/TiO₂-HNSs possess similar intrinsic properties and comparable surface areas. Therefore, the higher photocatalytic activity of the Au/TiO₂-3DHNSs can be mainly attributed to the multiple light scattering resulting from its unique 3DHNS structure. We believe that this result will be of great interest because the effect of multiple light scattering was previously found to play only a minor part in the photocatalytic activity of TiO₂ with ordered macroporous structure.^[7c,f] The enhanced light scattering in 3DHNSs compared to TiO₂ ordered macroporous materials may be due to its highly nanoporous structure, which consists of ordered voids both inside and outside the ultrathin shell HNSs.

In conclusion, we have demonstrated the construction of three-dimensional ordered assembly of thin-shell Au/TiO₂ HNSs from SiO₂ NSs and TNDs. The designed Au/TiO₂-3DHNS materials exhibit a high surface area, photonic behavior, and enhanced light scattering effects. These unique properties permit Au/TiO₂-3DHNSs to absorb visible light with great efficiency. As a result, the designed photocatalysts exhibit significantly enhanced visible-light-driven photocatalytic activity compared to conventional Au/TiO₂ nanopowders. Given that the photonic behavior of the 3DHNS structure can be tuned by varying the size of SiO₂ core while maintaining a high surface area, we believe that the 3DHNS structure not only offers a powerful tool for the construction of efficient photocatalysts, but will also have

a wide impact in all applications where high surface area and effective light absorption are essential.

Received: January 28, 2014

Published online: April 15, 2014

Keywords: gold · nanostructures · ordered assembly · photocatalysis · titanium dioxide

- [1] a) X. B. Chen, S. H. Shen, L. J. Guo, S. S. Mao, *Chem. Rev.* **2010**, *110*, 6503; b) X. Wang, K. Maeda, A. Thomas, K. Takanabe, G. Xin, J. M. Carlsson, K. Domen, M. Antonietti, *Nat. Mater.* **2009**, *8*, 76; c) I. Tsuji, H. Kato, A. Kudo, *Angew. Chem.* **2005**, *117*, 3631; *Angew. Chem. Int. Ed.* **2005**, *44*, 3565; d) P. Wang, B. Huang, X. Qin, X. Zhang, Y. Dai, J. Wei, M. H. Whangbo, *Angew. Chem.* **2008**, *120*, 8049; *Angew. Chem. Int. Ed.* **2008**, *47*, 7931; e) C. T. Dinh, T. D. Nguyen, F. Kleitz, T. O. Do, *Chem. Commun.* **2011**, *47*, 7797.
- [2] a) A. Fujishima, K. Honda, *Nature* **1972**, *238*, 37; b) H. G. Yang, C. H. Sun, S. Z. Qiao, J. Zou, G. Liu, S. C. Smith, H. M. Cheng, G. Q. Lu, *Nature* **2008**, *453*, 638; c) C. T. Dinh, T. D. Nguyen, F. Kleitz, T. O. Do, *ACS Nano* **2009**, *3*, 3737; d) M. R. Hoffmann, S. T. Martin, W. Choi, D. W. Bahnemann, *Chem. Rev.* **1995**, *95*, 69; e) X. Chen, S. S. Mao, *Chem. Rev.* **2007**, *107*, 2891; f) E. J. W. Crossland, N. Noel, V. Sivaram, T. Leijtens, J. A. Alexander-Webber, H. J. Snaith, *Nature* **2013**, *495*, 215.
- [3] a) B. O'Regan, M. Gratzel, *Nature* **1991**, *353*, 737; b) S. C. Hayden, N. K. Allam, M. A. El-Sayed, *J. Am. Chem. Soc.* **2010**, *132*, 14406; c) J. Ryu, S. H. Lee, D. H. Nam, C. B. Park, *Adv. Mater.* **2011**, *23*, 1883.
- [4] a) R. Asahi, T. Morikawa, T. Ohwaki, K. Aoki, Y. Taga, *Science* **2001**, *293*, 269; b) S. U. M. Khan, M. Al-Shahry, W. B. Ingler, *Science* **2002**, *297*, 2243; c) S. Hoang, S. Guo, N. T. Hahn, A. J. Bard, C. B. Mullins, *Nano Lett.* **2012**, *12*, 26; d) X. Chen, L. Liu, P. Y. Yu, S. S. Mao, *Science* **2011**, *331*, 746.
- [5] a) Y. Tian, T. Tatsuma, *J. Am. Chem. Soc.* **2005**, *127*, 7632; b) S. Linic, P. Christopher, D. B. Ingram, *Nat. Mater.* **2011**, *10*, 911; c) Q. Zhang, D. Q. Lima, I. Lee, F. Zaera, M. Chi, Y. Yin, *Angew. Chem.* **2011**, *123*, 7226; *Angew. Chem. Int. Ed.* **2011**, *50*, 7088; d) L. Liu, S. Ouyang, J. Ye, *Angew. Chem.* **2013**, *125*, 6821; *Angew. Chem. Int. Ed.* **2013**, *52*, 6689; e) C. Yu, G. Li, S. Kumar, H. Kawasaki, R. Jin, *J. Phys. Chem. Lett.* **2013**, *4*, 2847; f) J. B. Priebe, M. Karnahl, H. Junge, M. Beller, D. Hollmann, A. Bruckner, *Angew. Chem.* **2013**, *125*, 11631; *Angew. Chem. Int. Ed.* **2013**, *52*, 11420; g) J. E. Yoo, K. Lee, M. Altomare, E. Selli, P. Schmuki, *Angew. Chem.* **2013**, *125*, 7662; *Angew. Chem. Int. Ed.* **2013**, *52*, 7514; h) Z. Bian, T. Tachikawa, P. Zhang, M. Fujitsuka, T. Majima, *J. Am. Chem. Soc.* **2014**, *136*, 458; i) C. Gomes Silva, R. Juarez, T. Marino, R. Molinari, H. Garcia, *J. Am. Chem. Soc.* **2011**, *133*, 595; j) S. T. Kochuveedu, Y. H. Jang, D. H. Kim, *Chem. Soc. Rev.* **2013**, *42*, 8467; k) A. Primo, A. Corma, H. Garcia, *Phys. Chem. Chem. Phys.* **2011**, *13*, 886; l) Y. C. Pu, G. Wang, K. D. Chang, Y. Ling, Y. K. Lin, B. C. Fitzmorris, C. M. Liu, X. Lu, Y. Tong, J. Z. Zhang, Y. J. Hsu, Y. Li, *Nano Lett.* **2013**, *13*, 3817; m) A. Tanaka, S. Sakaguchi, K. Hashimoto, H. Kominami, *ACS Catal.* **2013**, *3*, 79.
- [6] a) S. Kim, A. N. Mitropoulos, J. D. Spitzberg, H. Tao, D. L. Kaplan, F. G. Omenetto, *Nat. Photonics* **2012**, *6*, 818; b) Z. Zhang, L. Zhang, M. N. Hedhili, H. Zhang, P. Wang, *Nano Lett.* **2013**, *13*, 14; c) O. Sánchez-Sobrado, G. Lozano, M. E. Calvo, A. S. Iglesias, L. M. L. Marzan, H. Miguez, *Adv. Mater.* **2011**, *23*, 2108; d) Y. Tan, W. Qian, S. Ding, Y. Wang, *Chem. Mater.* **2006**, *18*, 3385.
- [7] a) M. Notomi, K. Yamada, A. Shinya, J. Takahashi, C. Takahashi, I. Yokohama, *Phys. Rev. Lett.* **2001**, *87*, 253902; b) Yu. A.

- Vlasov, M. O'Boyle, H. F. Hamann, S. J. McNab, *Nature* **2005**, *438*, 65; c) J. I. L. Chen, G. Von Freymann, S. Y. Choi, V. Kitaev, G. A. Ozin, *Adv. Mater.* **2006**, *18*, 1915; d) J. I. L. Chen, G. Von Freymann, V. Kitaev, G. A. Ozin, *J. Am. Chem. Soc.* **2007**, *129*, 1196; e) J. I. L. Chen, E. Loso, N. Ebrahin, G. A. Ozin, *J. Am. Chem. Soc.* **2008**, *130*, 5420; f) F. Sordello, C. Duc, V. Maurino, C. Minero, *Chem. Commun.* **2011**, *47*, 6147; g) S. Nishimura, N. Abrams, B. A. Lewis, L. I. Halaoui, T. E. Mallouk, K. D. Benkstein, J. van de Lagemaat, A. J. Frank, *J. Am. Chem. Soc.* **2003**, *125*, 6306; h) X. Q. Chen, J. H. Ye, S. X. Ouyang, T. Kako, Z. S. Li, Z. G. Zou, *ACS Nano* **2011**, *5*, 4310; i) M. Y. Tsang, N. E. Pridmor, L. J. Gillie, Y. H. Chou, R. Brydson, R. E. Douthwaite, *Adv. Mater.* **2012**, *24*, 3406; j) S. Meng, D. Li, X. Zheng, J. Wang, J. Chen, J. Fang, Y. Shao, X. Fu, *J. Mater. Chem. A* **2013**, *1*, 2744; k) M. Wu, Y. Li, Z. Deng, B. L. Su, *ChemSusChem* **2011**, *4*, 1481; l) J. Liu, G. Liu, M. Li, W. Shen, Z. Liu, J. Wang, J. Zhao, L. Jiang, Y. Song, *Energy Environ. Sci.* **2010**, *3*, 1503.
- [8] a) B. T. Holland, C. F. Blanford, A. Stein, *Science* **1998**, *281*, 538; b) A. Stein, B. E. Wilson, S. G. Rudisill, *Chem. Soc. Rev.* **2013**, *42*, 2763; c) G. von Freymann, V. Kitaev, B. V. Lotsch, G. A. Ozin, *Chem. Soc. Rev.* **2013**, *42*, 2528.
- [9] a) C. T. Dinh, Y. Seo, T. D. Nguyen, F. Kleitz, T. O. Do, *Angew. Chem.* **2012**, *124*, 6712; *Angew. Chem. Int. Ed.* **2012**, *51*, 6608; b) C. T. Dinh, M. H. Pham, F. Kleitz, T. O. Do, *J. Mater. Chem. A* **2013**, *1*, 13308.
- [10] J. D. Henao, Y. W. Suh, J. K. Lee, M. C. Kung, H. H. Kung, *J. Am. Chem. Soc.* **2008**, *130*, 16142.
- [11] a) Y. Wu, H. Liu, J. Zhang, F. Chen, *J. Phys. Chem. C* **2009**, *113*, 14689; b) N. Kruse, S. Chenakin, *Appl. Catal. A* **2011**, *391*, 367.
- [12] B. M. Reddy, B. Chowdhury, P. G. Smirniotis, *Appl. Catal. A* **2001**, *219*, 53.
- [13] S. J. Gregg, K. S. W. Sing, *Adsorption, Surface Area and Porosity*, Academic Press, London, **1982**.
- [14] a) D. M. Antonelli, J. Y. Ying, *Angew. Chem.* **1995**, *107*, 2202; *Angew. Chem. Int. Ed. Engl.* **1995**, *34*, 2014; b) T. Fröschl, U. Hormann, P. Kubiak, G. Kucerova, M. Planzel, C. K. Weiss, R. J. Behm, N. Husing, U. Kaiser, K. Landfester, M. W. Mehrens, *Chem. Soc. Rev.* **2012**, *41*, 5313; c) A. A. Ismail, D. W. Bahnemann, *J. Mater. Chem.* **2011**, *21*, 11686; d) K. E. Shopsowitz, A. Stahl, W. Y. Hamad, M. J. MacLachlan, *Angew. Chem.* **2012**, *124*, 6992; *Angew. Chem. Int. Ed.* **2012**, *51*, 6886.
- [15] a) F. Marlow, Muldarisnur, P. Sharifi, R. Brinkmann, C. Mendive, *Angew. Chem.* **2009**, *121*, 6328; *Angew. Chem. Int. Ed.* **2009**, *48*, 6212; b) J. E. G. J. Wijnhoven, W. L. Vos, *Science* **1998**, *281*, 802.

Supporting Information

© Wiley-VCH 2014

69451 Weinheim, Germany

Three-Dimensional Ordered Assembly of Thin-Shell Au/TiO₂ Hollow Nanospheres for Enhanced Visible-Light-Driven Photocatalysis**

*Cao-Thang Dinh, Hoang Yen, Freddy Kleitz, and Trong-On Do**

anie_201400966_sm_miscellaneous_information.pdf

Experimental Section

Chemicals: Titanium butoxide (TB), benzyl alcohol (BA), oleylamine (OM), benzyl ether, tetraethylammonium (TEA) hydroxide, Tetraethylorthosilicate (TEOS), polyethylenimine (PEI), ammonium hydroxide, tetrachloroauric(III) acid, silica colloids (Ludox AS-40), and sodium borohydride were purchased from Aldrich. All of the reagents were used without further purification.

Synthesis of titanate nanodisks (TNDs): The synthesis of water-soluble TNDs was based on our previous work.^[1] Briefly, 2g of TB, 12 g of OM, 12g of BA and 30g of benzyl ether were added to a 100-mL round-bottom flask. The reaction mixture was heated to 190 °C at the heating rate 5 °C/min under nitrogen flow. After 20 h, the reaction was stopped and cooled down to room temperature. After addition of excess absolute ethanol, the TNDs were obtained and were then re-dispersed in toluene and re-precipitated with ethanol. This process was repeated three times to remove the un-reacted reagents. After that, the as-synthesized TNDs were treated with tetraethyl ammonium hydroxide to obtain TEA-TNDs. Typically, 5 mmol of as-synthesized TNDs (according to Ti atom) were dispersed in a mixture of TEAOH (15 mmol), ethanol (15 ml) and water (15 ml). The mixture was stirred overnight at room temperature. An excess of acetone was added to the obtained clear solution to precipitate TNDs. The precipitate was then washed several times with acetone and finally dispersed in 10 ml of water.

Synthesis of silica nanospheres: SiO₂ NSs were synthesized following the Stöber synthesis.^[2] TEOS (45 ml) was added to a mixture of ethanol (750 ml), H₂O (60 ml) and ammonia solution (40 ml, 28wt %). After stirring for 4 h at room temperature, the precipitated silica NSs were separated by centrifugation and washed 3 times with ethanol. The SiO₂ NSs were then re-dispersed in 100 ml of H₂O.

Coating SiO₂ NSs with TNDs: SiO₂ NSs were coated with TNDs using a layer-by-layer deposition technique.^[3] Typically, 5 g of SiO₂ NSs was dispersed in 200 ml of H₂O containing 0.2 g of PEI. The suspension was stirred for 30 min to ensure the saturated adsorption of PEI on the surface of the SiO₂. Excess PEI was removed by centrifugation. The obtained PEI-coated SiO₂ was then redispersed in 200 ml of H₂O. After that, 10 ml solution of TNDs (containing 0.1g TNDs) was gradually added to the SiO₂ NS suspension under stirring. Formation of flocculated aggregates in the mixture, which is caused by the electrostatic interaction of the negatively charged TNDs and positively charged PEI on SiO₂ surface, was observed after the addition of TND solution. The resulting material was then recovered by centrifugation and washing process. The above procedure was repeated for a 12 cycles to obtain TND-PEI/SiO₂ NSs.

Synthesis of Au/TiO₂-3DHNSs: The obtained TND-PEI/SiO₂ NSs were re-dispersed in 200 ml of H₂O. To this mixture was added 10 ml of HAuCl₄ solution (15 mM). The resulting mixture was stirred for 60 min to ensure the adsorption of AuCl₄⁻ on the TND-PEI/SiO₂ NSs. After that, the mixture was centrifuged with the speed of 1500 round per minute for 60 min to obtain 3D ordered assembly of TND-PEI-AuCl₄⁻/SiO₂ NSs. The obtained precipitate was dried at 60 °C overnight and then calcined at 550 °C (ramp rate of 2 °C/min) for 4 hours to obtain Au/TiO₂/SiO₂ 3D ordered assembly. The SiO₂ NSs were then removed from the composite by treating the

materials with 100 ml of NaOH solution (2M) at 80 °C for 2h. The obtained Au/TiO₂-3DHNSs were washed several times with water and then dried at 60 °C overnight.

Synthesis of TiO₂-3DHNSs, Au/TiO₂-HNSs (without 3D ordered assembly structure), and Au/TiO₂-P25: The TiO₂-3DHNSs were synthesized in a similar procedure to that of Au/TiO₂-3DHNSs except that Au precursor (AuCl₄⁻) was not used to be absorbed on TND-PEI/SiO₂ NSs. The Au/TiO₂-HNSs without 3DOA structure was synthesized as follows: the TND-PEI-AuCl₄⁻/SiO₂ NSs (see the synthesis of Au/TiO₂-3DHNSs) were first mixed with silica colloids (Ludox AS40). The mixture was then dried and calcined at 550 °C for 4h. The silica added and SiO₂ NSs were then removed by NaOH 2M at 80 °C for 2h. The Au/TiO₂-P25 was synthesized using a chemical reduction method. Briefly, TiO₂-P25 nanopowder was dispersed in a solution containing HAuCl₄. The pH of the solution was then adjusted to 8 using a dilute ammonia solution and was stirred for 1 h. To the obtained mixture was added a fresh prepared sodium borohydride solution under stirring condition. The resulted Au/TiO₂-P25 was then washed several time with water and dried at 60 °C overnight.

Characterizations: Transmission electron microscopy (TEM) images of the samples were obtained on a JOEL JEM 1230 operated at 120kV. High resolution TEM (HRTEM) images were performed on Philips G2 F30 Tecnai instrument operated at 300kV. Scanning electron microscopy (SEM) images were obtained on a JEOL 6360 instrument operated at 15 kV. Powder X-ray diffraction (XRD) patterns of the samples were obtained on a Bruker SMART APEXII X-ray diffractometer equipped with a Cu K α radiation source ($\lambda=1.5418 \text{ \AA}$). X-ray photoelectron spectroscopy (XPS) measurements carried out in an ion-pumped chamber (evacuated to 10⁻⁹ Torr) of a photoelectron spectrometer (Kratos Axis-Ultra) equipped with a focused X-ray source (Al K α , $h\nu = 1486.6 \text{ eV}$). The UV-vis spectra were recorded on a Cary 300 Bio UV-visible spectrophotometer. N₂ adsorption-desorption isotherms of the samples were measured at -196 °C using Quantachrome Autosorb-1 MP analyzer. Before the measurements, the samples were outgassed under vacuum for 6 h at 110 °C.

Photocatalytic decomposition of isopropanol: The photocatalytic reactions were carried out in a gas-tight 30 ml Pyrex reaction cell at ambient temperature and atmospheric pressure. In a typical photocatalytic experiment, 30 mg of photocatalysts was spread uniformly in the reaction cell with an irradiation area of 4 cm². The reaction cell was then evacuated, and filled with fresh synthetic air. After that, a certain amount of gaseous iso-propanol was injected into the reactor. Prior to light irradiation, the reaction cell was kept in dark for 4 h to ensure that an adsorption desorption equilibrium of isopropanol on the surface of the photocatalysts was established. Then, the reaction cell was illuminated with a 300W Xe arc lamp equipped with an UV-cutoff filter ($\geq 420 \text{ nm}$) for 10 hours or with an UV Hg lamp (wavelength of 365 nm) for 4 hours. The CO₂ gas generated was analysed by a gas chromatography equipped with TCD detector and carboxen-1010 capillary column.

References:

- 1) Dinh, C. T.; Seo, Y.; Nguyen, T. D.; Kleitz, F.; Do, T. O. *Angew. Chem. Int. Ed.* **2012**, *51*, 6608.
- 2) Stober, W.; Fink, A.; Bohn, E. *J. Colloid Interface Sci.* **1968**, *26*, 62.
- 3) Wang, L.; Sasaki, T.; Ebina, Y.; Kurashima, K.; Watanabe, M. *Chem. Mater.* **2002**, *14*, 4827.

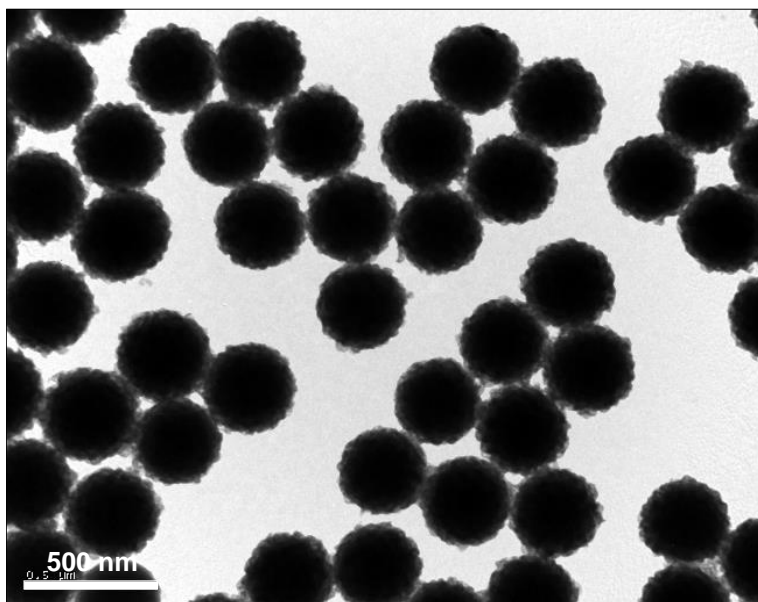


Figure S1. TEM image of TND-PEI-AuCl₄⁻/SiO₂ NSs

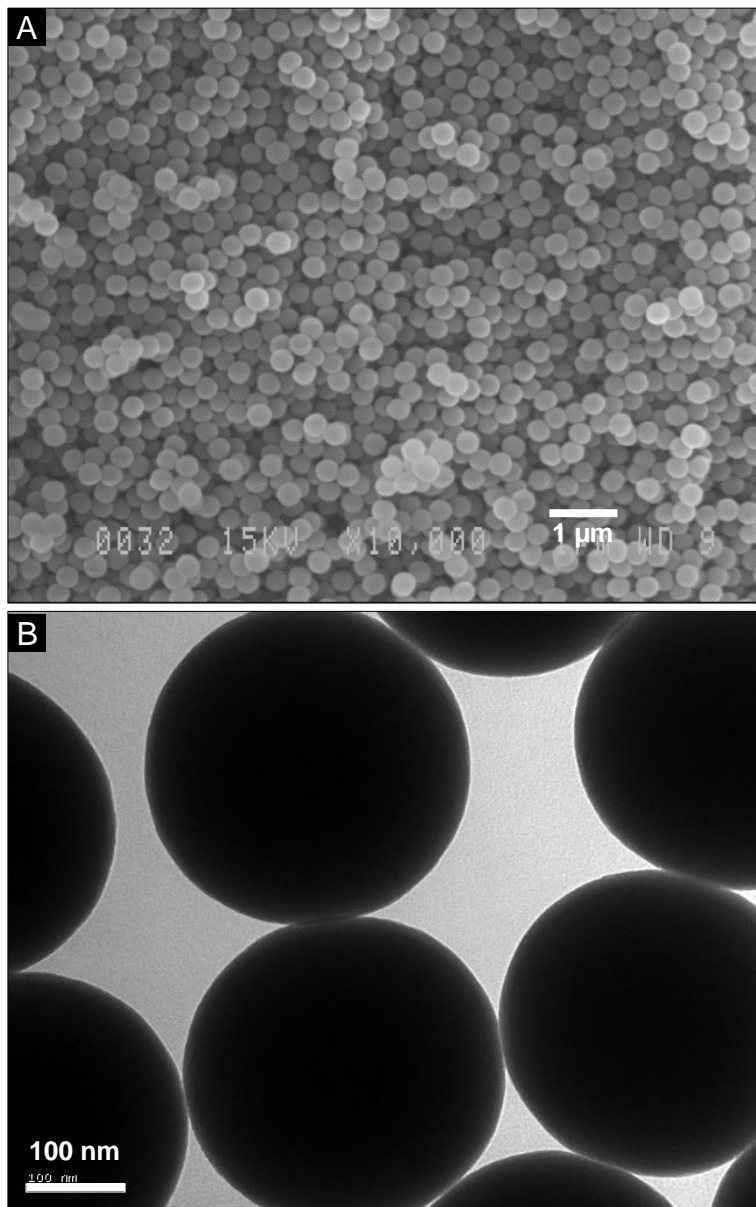


Figure S2. (A) SEM image showing the uniform size of SiO₂ NSs. (B) TEM image showing the smooth surface of SiO₂ NSs.

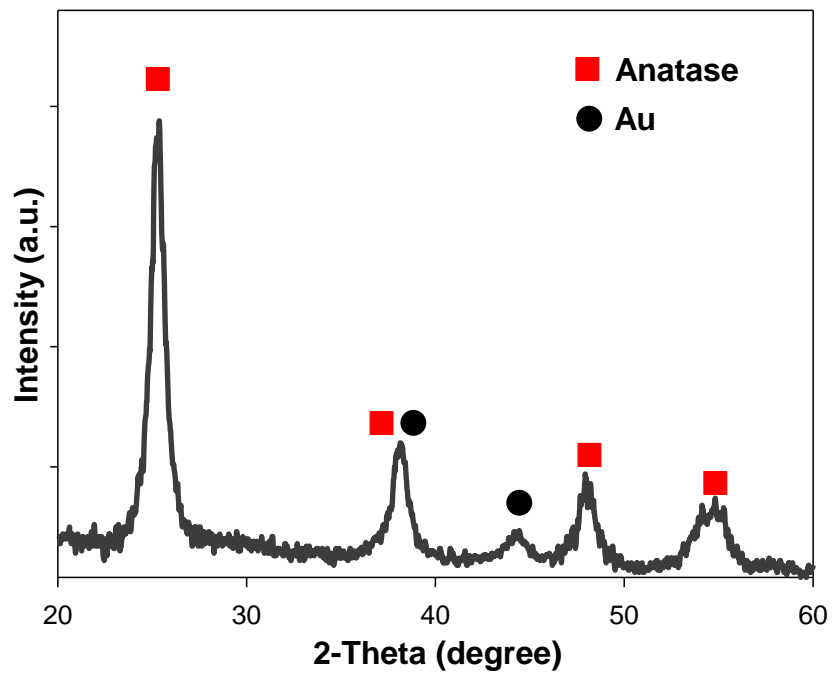


Figure S3. XRD patter of Au/TiO₂-3DHNSs.

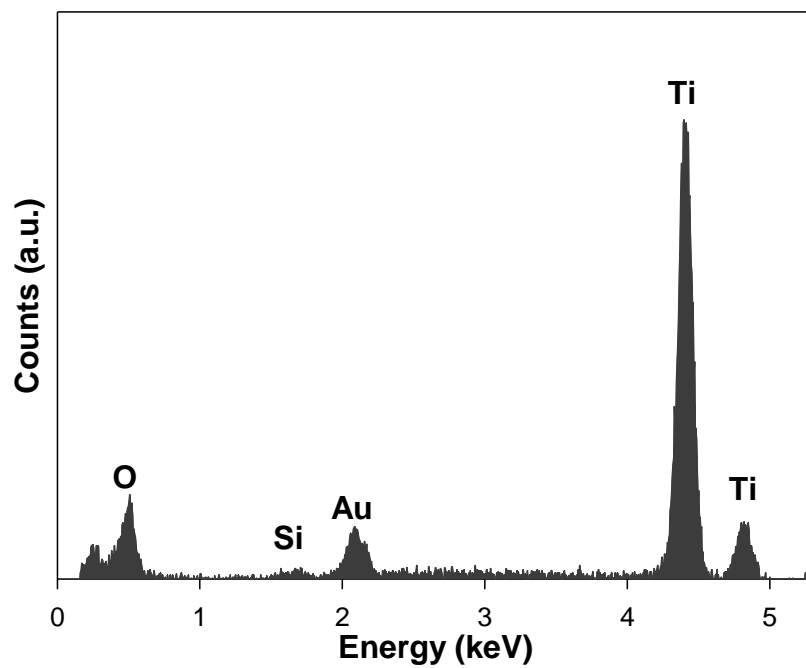


Figure S4. EDX spectrum of Au/TiO₂-3DHNSs confirming the presence of Au and Ti in the sample. It can be also observed that the amount of silica remained in the sample is negligible.

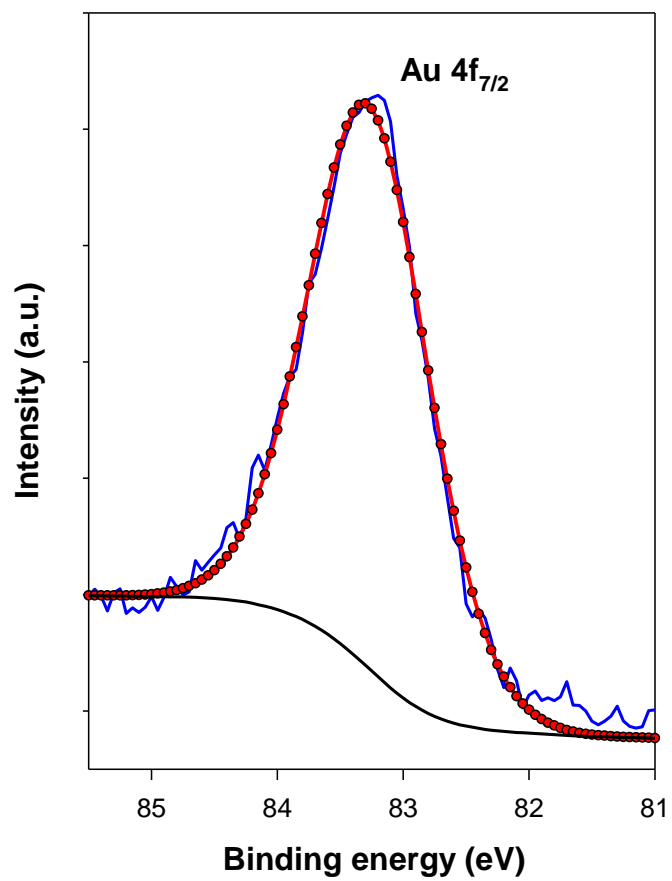


Figure S5. Au 4f_{7/2} XPS spectrum of Au/TiO₂-3DHNSs.

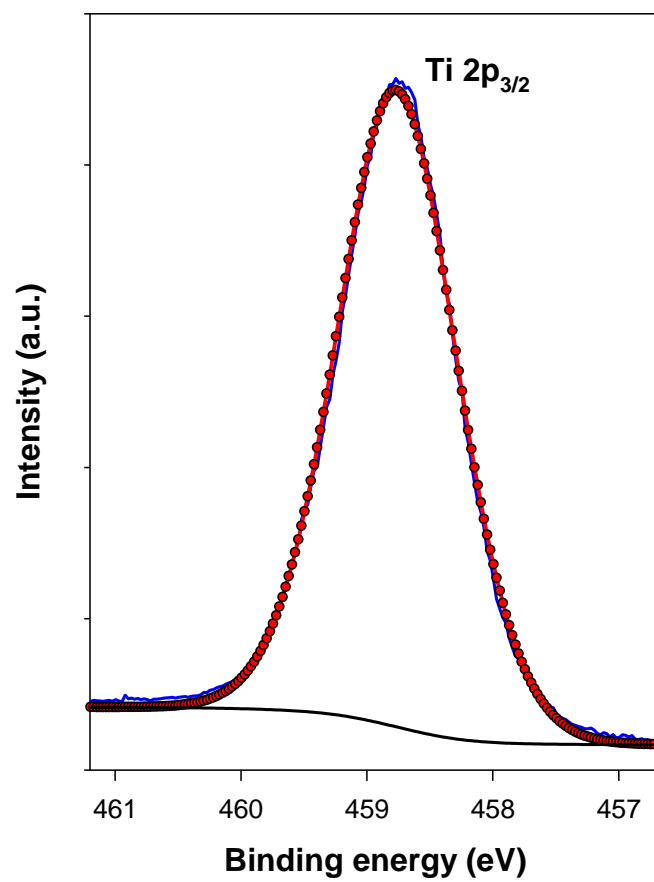


Figure S6. Ti 2p_{3/2} XPS spectrum of Au/TiO₂-3DHNSs.

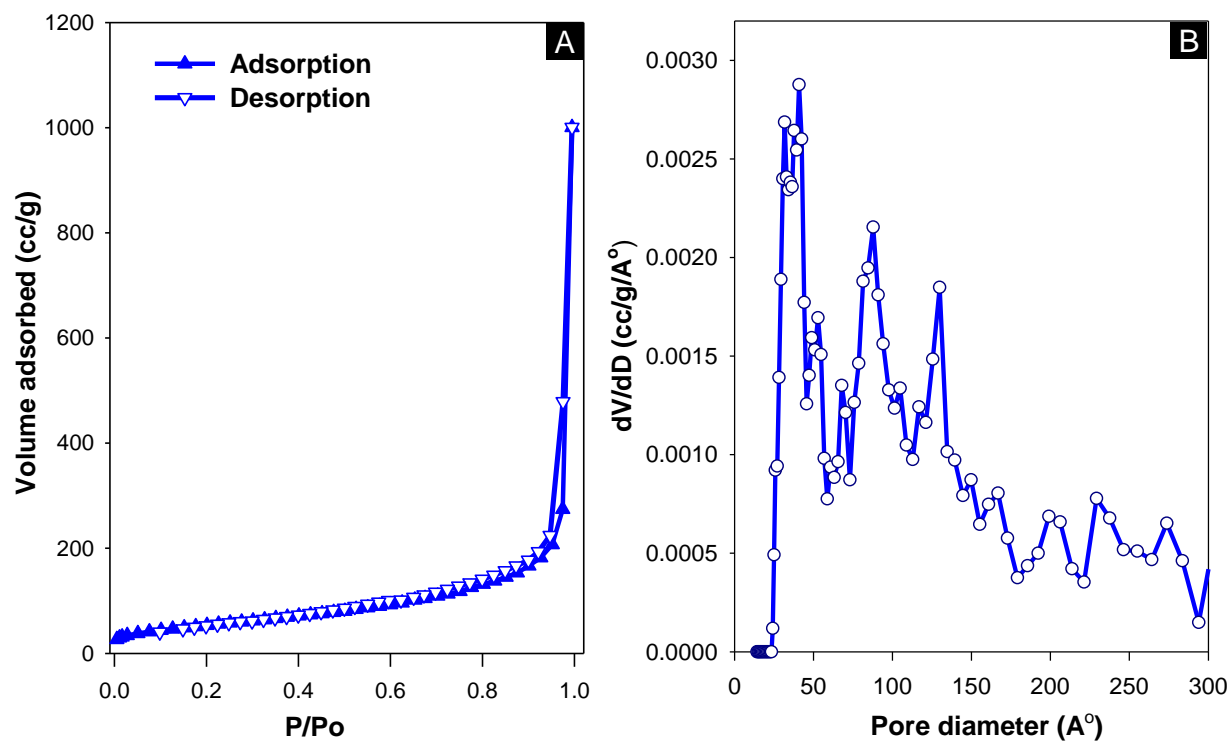


Figure S7. Nitrogen sorption isotherms of Au/TiO₂-3DHNSs (A), and the respective NLDFT pore size distribution calculated from the adsorption branch (B).

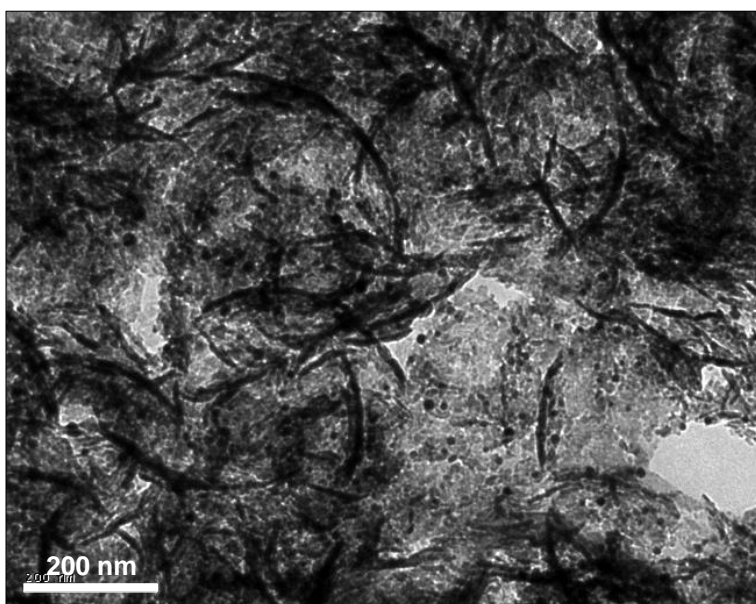


Figure S8. TEM image of Au/TiO₂-3DHNSs crushed.

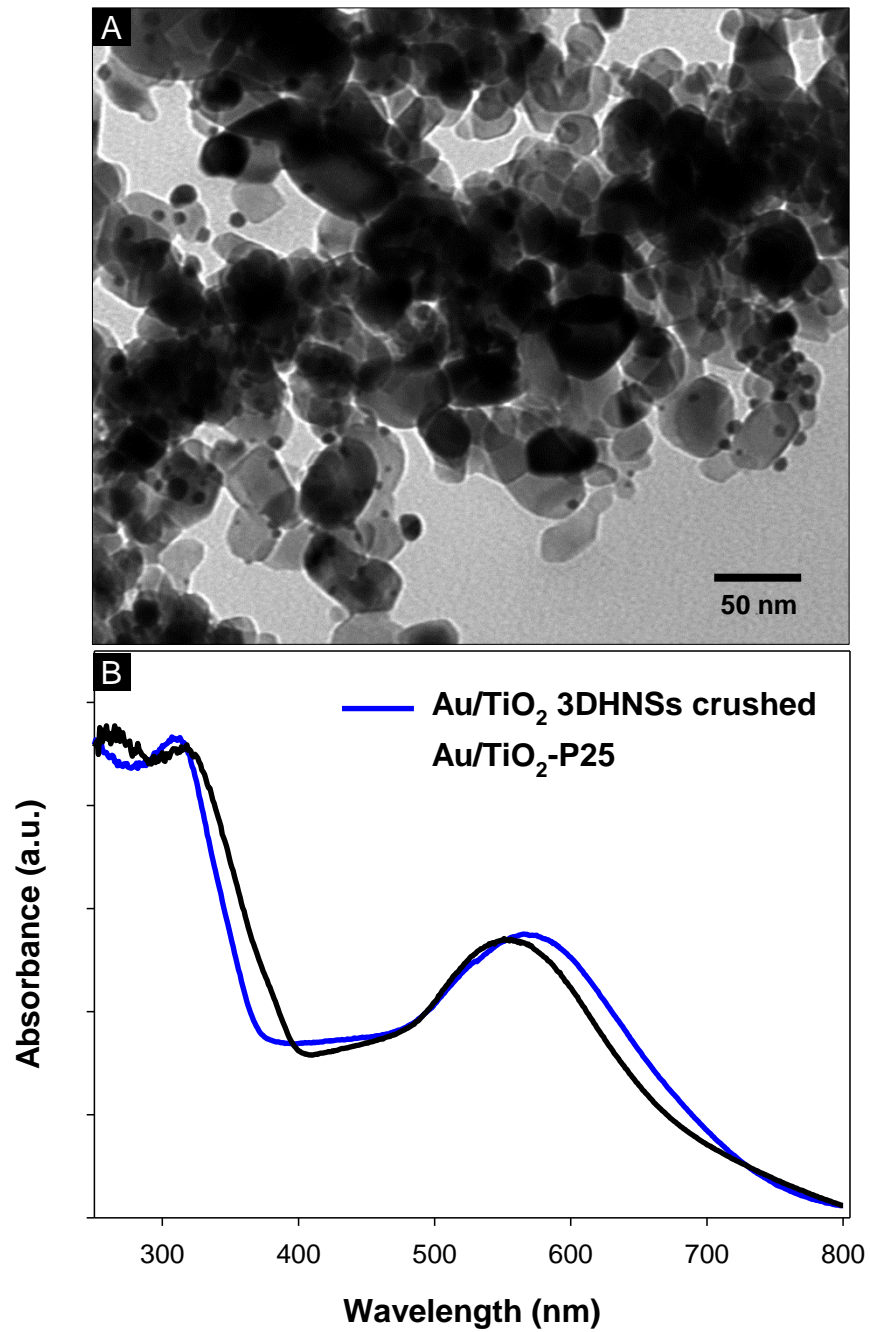


Figure S9. (A) TEM image of Au/TiO₂-P25 showing the presence of Au nanoparticles with the size from 8-15 nm. (B) UV-vis absorption spectra of Au/TiO₂-P25 in comparison to that of Au/TiO₂-3DHNSs crushed sample.

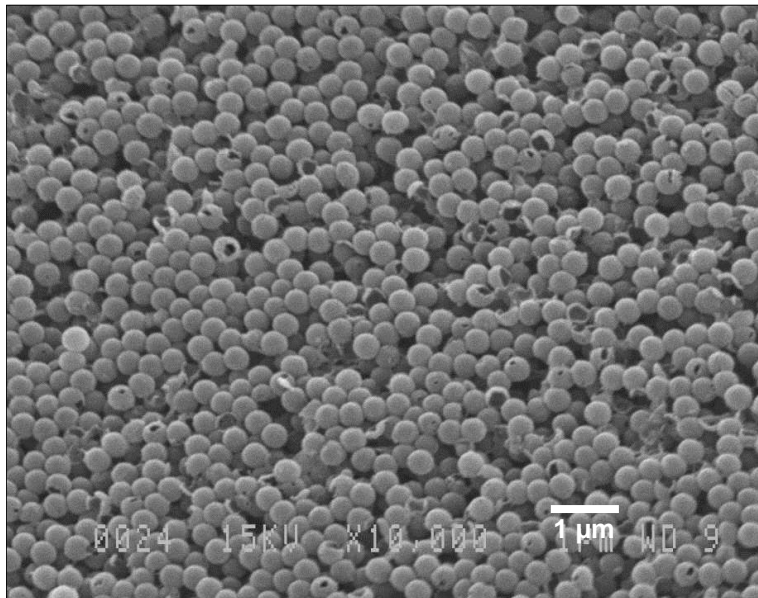


Figure S10. SEM image of Au/TiO₂-HNSs without 3D ordered assembly structure.